Future scenarios for earthquake and flood risk in Eastern Europe and Central Asia

Murnane, Rick; Daniell, James E.; Schafer, A.M.; Ward, P.J.; Winsemius, H.C.; Simpson, A.; Tijssen, A.; Toro, Joaquin

published in
Earth's Future
2017

DOI (link to publisher)
10.1002/2016EF000481

document version
Publisher's PDF, also known as Version of record

AGU PUBLICATIONS

Earth's Future

RESEARCH ARTICLE
10.1002/2016EF000481

Future scenarios for earthquake and flood risk in Eastern Europe and Central Asia

R. J. Murnane[1], J. E. Daniell[2], A. M. Schäfer[2], P. J. Ward[3], H. C. Winsemius[4], A. Simpson[1], A. Tijssen[5], and J. Toro[5]

[1]GFDRR, World Bank, Washington, D.C., USA, [2]Karlsruhe Institute of Technology, Geophysical Institute, CEDIM, Karlsruhe, Germany, [3]Institute for Environmental Studies (IVM), Vrije Universiteit Amsterdam, Amsterdam, Netherlands, [4]Deltares, Delft, Netherlands, [5]World Bank, Washington, D.C., USA

Key Points:
- Future changes in modeled earthquake risk vary with socioeconomic pathway
- Future changes in modeled flood risk vary with global climate model, greenhouse gas emission scenario, and socioeconomic pathway
- Relative change in population affected by flooding can inform the selection of countries for further detailed risk analysis

Corresponding author:
R.J. Murnane, rmurnane@worldbank.org

Citation:
Murnane, R. J., J. E. Daniell, A. M. Schäfer, P. J. Ward, H. Winsemius, A. Simpson, A. Tijssen, and J. Toro (2017), Future scenarios for earthquake and flood risk in Eastern Europe and Central Asia, *Earth's Future*, *5*, doi:10.1002/2016EF000481.

Received 24 OCT 2016
Accepted 13 JUN 2017
Accepted article online 20 JUN 2017

Abstract We report on a regional flood and earthquake risk assessment for 33 countries in Eastern Europe and Central Asia. Flood and earthquake risk were defined in terms of affected population and affected gross domestic product (GDP). Earthquake risk was also quantified in terms of fatalities and capital loss. Estimates of future population and GDP affected by earthquakes vary significantly among five shared socioeconomic pathways that are used to represent population and GDP in 2030 and 2080. There is a linear relationship between the future relative change in a nation's exposure (population or GDP) and its future relative change in annual average population or GDP affected by earthquakes. The evolution of flood hazard was quantified using a flood model with boundary conditions derived from five different general circulation models and two representative concentration pathways, and changes in population and GDP were quantified using two shared socioeconomic pathways. There is a nonlinear relationship between the future relative change in a nation's exposure (population or GDP) and its future relative change in its annual average population or GDP affected by floods. Six regions can be defined for positive and negative relative change in population that designate whether climate change can temper, counter, or reinforce relative changes in flood risk produced by changes in population or exposure. The departure from the one-to-one relationship between a relative change in a nation's population or GDP and its relative change in flood risk could be used to inform further efforts at flood mitigation and adaptation.

Plain Language Summary Floods and earthquakes affect the economy and population of countries in Eastern Europe and Central Asia. Future changes in these countries' economies and population will change the impacts of floods and earthquakes. In addition, future changes in climate will change how often flooding occurs. We assume that earthquake occurrence won't change with climate changes. We show how much the economies and populations of these countries are affected by floods and earthquakes in 2015, 2030 and 2080. However, as we don't know for certain how the economies, population and climate will change in the future, we show result for a variety of scenarios for future economies, population and climate. We assess how future changes in the economy and population affect future flood risk using changes in earthquake risk, and assume the remaining change is caused by changes in climate. We suggest that for some countries the population affected by floods can increase even with a decrease in population, or the population affected by floods and decrease even with an increase in population, if the future change in flood hazard is sufficiently large.

1. Introduction

Natural disasters disproportionately affect developing countries. The death and destruction caused by these events can have an impact on the gross domestic product (GDP) of developing countries that is 20 times larger than their impact on developed, industrialized countries [*Sanghi et al.,* 2011]. An example of the large impacts of flooding on GDP can be drawn from the 2014 floods in Serbia (SRB). The flooding affected approximately 50,000 people and caused 54 fatalities [*Guha-Sapir et al*., 2016]. Damage and losses totaled over $US 2 billion [*Guha-Sapir et al*., 2016], approximately 5% of the predisaster estimates of Serbia's 2014 GDP of $44 billion [*World Bank*, 2017]. The incremental impact of the flooding was estimated to lower

Table 1. Examples of Significant Earthquakes and Floods in Eastern Europe and Central Asia

Country	Year	Event
Greece (GRC)	ca. 365	Earthquake destroys many cities on Crete, tsunami strikes eastern and southern Mediterranean [*Stiros*, 2001].
Turkey (TUR)	ca. 526	Earthquake and subsequent fire destroys Antioch and kills about 250,000 people [*Sbeinati et al*., 2005].
Turkey (TUR)	1509	Earthquake damages Constantinople/Istanbul causing 1500–5000 deaths [*Ambraseys*, 2009].
Azerbaijan (AZE)	1667	Earthquake causes up to 80,000 deaths [*Lomnitz*, 1974]
Croatia (HRV)	1667	Earthquake near Dubrovnik causes approximately 4000 deaths [*Ambraseys*, 2009; *Albini*, 2015].
Armenia (ARM)	1679	Earthquake near Yerevan causes between 1500 and 8000 deaths [*Ambraseys*, 2009].
Romania (ROU)	1802	One of Romania's strongest historical earthquakes causes extensive damage [*Constantin et al*., 2011].
Russian Federation (RUS)	1824	Worst historical flooding of St. Petersburg [*Barabanova*, 2014]
Hungary (HUN)	1838	Floods extensively damaged Pest [*Tenk and David*, 2015].
Romania (ROU), Moldova/USSR (MDA)	1940	Vrancea earthquake extensively damages Bucharest and Chisinau [*Alcaz et al*., 2008].
Turkmen/USSR (TKM)	1948	Earthquake near Ashgabat likely killed over 100,000 people, ca. 50% of the population of the city [*Daniell et al*., 2011].
Macedonia/Yugoslavia (MKD)	1962 and 1963	Earthquake destroys nearly 80% of Skopje, 1 year after large flooding throughout the city *[Sinadinovski and McCue*, 2013; *Daniell et al*., 2016]
Uzbek/USSR (UZB)	1966	Earthquake causes ~60% homelessness in Tashkent [*Daniell et al*., 2011, *UzReport*, 2017]
Tajikistan (TJK)	1998	Flooding causes over 100 deaths and damage equal to ~5% of GDP [*World Bank*, 1998].

The three letters in parentheses are the ISO Alpha-3 country code for a country.

Serbia's 2014 economic growth by nearly 1% [*European Union, United Nations and World Bank*, 2014]. The 2014 flooding in Serbia is only one example of numerous historical natural disasters in Eastern Europe and Central Asia (ECA). A selection of past events is offered in Table 1.

Future changes in climate are expected to alter the distribution and intensity of extreme weather. For example, as stated in the Intergovernmental Panel on Climate Change (IPCC) AR5 Summary for Policymakers, by the end of this century, it is very likely that over most of the mid-latitude land masses and over wet tropical regions, extreme precipitation events will become more frequent and intense, and that heat waves will occur with a higher frequency and duration [*IPCC*, 2013]. Such changes will in some cases, for example, produce wetter wet periods and drier dry periods [e.g., *Liu and Allan*, 2013] and result in a greater risk for floods and droughts [*Trenberth*, 2011]. A recent report concluded that unless appropriate actions are taken, approximately 100 million people could be pushed into extreme poverty by 2030 as a result of climate change [*Hallegatte et al*., 2016]. Without serious efforts to manage and reduce natural disaster risk, the impacts from future extreme events will likely continue to grow [*Global Facility for Disaster Reduction and Recovery* (*GFDRR*), 2016].

In response to the potential for future impacts (e.g., fatalities, damaged infrastructure, lower GDP) from natural disasters, a variety of international organizations, such as the World Bank, African Risk Capacity, United Nations International Strategy for Disaster Reduction, and the European Union, are interested in promoting disaster risk management programs and developing financial products that allow developing countries to be better protected against, and more quickly respond to and recover from, natural disasters. The financial products include multicountry risk pools such as the Caribbean Catastrophe Risk Insurance Facility and the Pacific Catastrophe Risk Assessment and Financing Initiative, and the MultiCat Program, a catastrophe bond

issuance platform that gives governments and other public entities access to international capital markets to insure themselves against the risk of natural disasters. A major component of these efforts to manage and respond to natural disasters is risk assessments.

Here we describe the results of a risk assessment project that examined earthquake and flood risk for 33 countries in the ECA region. The project was initiated by the GFDRR and the World Bank and focused on current and future earthquake and flood risk to the population and GDP of countries in the ECA region. In addition, the assessment estimated the risk of capital loss and fatalities from earthquakes. The risk assessments provide first-order estimates of the spatial distribution of flood and earthquake risk and how it could evolve over time. The results from the risk assessment will be used to inform governments and decision makers of the countries of their earthquake and flood risk and to facilitate discussions on how they can become more resilient to both current and future risk.

2. Methods

A useful way to characterize natural disaster risk is to consider the three basic components that, when combined, turn an extreme event into a natural disaster. The impact of an extreme event can be described using the three sides of the "risk triangle" [*Crichton*, 1999]: exposure, vulnerability, and hazard. The area of the triangle schematically represents the impact from an event such as monetary loss or casualties. In most cases, an increase in the amount of exposure, the vulnerability of the exposure, or the intensity of the hazard will result in an event having a larger impact. This is represented by an increase of the triangle's area. Decreasing the amount of exposure and/or reducing its vulnerability will reduce the impact of an event. There are situations where these generalizations do not hold. For example, if an earthquake causes complete destruction, then the impact of a more intense event will be the same. Or, an extreme flood could destroy both well-built and poorly built structures. In practice, natural hazard risk is often determined using a catastrophe risk model that accounts for the hazard, exposure, and vulnerability [*Murnane et al*., 2016]. The hazard is usually characterized using a catalog of hypothetical events whose aggregate statistics (e.g., frequency, intensity, size, distribution, etc.) are consistent with the historical record and theory. The user often provides the exposure data. The vulnerability functions must be consistent with information provided by hazard and exposure components.

The impacts from each event are used to determine a variety of risk metrics such as annual average loss (AAL). One definition for AAL is that it equals T_X/N_X, where T_X is the total of losses that occur over a number of years, N_X, and X denotes whether the losses and number of years are from either the historical record or modeled losses. If the losses are from the historical record, then they should be corrected for inflation and changes in exposure. For some perils, such as earthquakes, which occur rarely and cause significant loss when they occur, the AAL derived from the historical record will likely be much less than the modeled AAL if a large event has not occurred within the time span of the historical record.

The AAL is only one view of risk and it provides little information on the frequency or magnitude of the loss events. To understand the ambiguity in frequency and magnitude, consider two end-member scenarios, each with an AAL = λ. One end-member scenario is a catalog with a single event that produced a loss of 10,000*λ. Another end-member scenario is a catalog with 10,000 events, each with a loss of λ. Each scenario produces the same AAL. Thus, other risk metrics, e.g., different return period losses derived from a probability of exceedance loss curve, are used to further characterize the risk. The return period is equal to $1/P$, where P is the annual probability of exceedance.

The two risk models used to estimate flood and earthquake risk followed different methodologies and had different vulnerability functions and hazard catalogues to estimate current risk in 2015 and future risk in 2030 and 2080. However, the flood and earthquake risk results for each time period are based on the same population and GDP exposure estimates. The hazard for the earthquake model is based on a stochastic catalog whereas the flood model hazard is derived using extreme value theory. The vulnerability functions used to estimate affected population and GDP are step functions that have a value of either 0 or 1 depending on ground motion intensity for earthquakes or inundation depth for floods. The earthquake model also includes more detailed, country-specific, vulnerability functions that are used to estimate capital loss and fatalities based on ground motion intensity. A reader interested in flood risk derived using flood damage functions and the same methodology can examine *Ward et al*. [2013].

Table 2. Overview of Shared Socioeconomic Pathways (SSPs)

Scenario	Description	GDP Per Capita Growth	Population Growth
SSP1	Sustainability	Medium to fast	Relatively low
SSP2	Current trends continue	Medium to slow	Medium
SSP3	Fragmented world	Slow	Relatively high
SSP4	Divided world	Low to medium/high	Mixed
SSP5	Conventional development	High	Peak and decline

SSP descriptions adapted from *O'Neill et al*. [2012].

Table 3. RCP and SSP Scenario Combinations Used to Estimate Future Flood Risk

RCP Scenario	SSP Scenario	Scenario Characterization
RCP4.5	SSP2	Cautiously optimistic
RCP8.5	SSP2	Present trends continue
RCP8.5	SSP3	Worst case

Five different shared socioeconomic pathways (SSPs) are used to define population and GDP exposure in 2030 and 2080. For background on the SSPs see *Ebi et al*. [2014]. An overview of the different SSPs is provided in Table 2. Earthquake hazard is assumed to be the same for all time periods.

Different climatic and socioeconomic conditions are used to explore the evolution of flood risk. Boundary conditions for the present day hydrological model were based on climate data from the European Union Water and Global Change (EU WATCH) project [*Weedon et al*., 2010]. Climate projections from five global climate models (GCMs) consistent with two representative concentration pathways (RCPs), RCP4.5 and RCP8.5, were used as 2030 and 2080 boundary conditions for the hydrological model. For a description of the RCPs see *van Vuuren et al*. [2011]. As shown in Table 3, a combination of two RCPs and two SSPs are used to estimate flood risk in this study.

For each country and province, flood and earthquake risks are quantified in terms of AAL and for a variety of return periods for the three snapshots at 2015, 2030, and 2080.

2.1. Earthquake Model

The earthquake model [*Daniell and Schaefer*, 2014] includes a hazard component that represents earthquake events as finite or point sources depending on magnitude and location, and vulnerability functions to estimate the loss caused by earthquake-induced ground motion that affects exposed people and assets. The earthquake hazard is quantified using a 10,000-year stochastic catalog of over 15.8 million synthetic earthquake events of at least magnitude 5 in the ECA region. The earthquake model contains 1437 source zones and 744 faults incorporating various regional and local studies over the past 30 years. The source zones are used to account for seismicity of unknown faults and for regions with low seismicity. The frequency and magnitude of earthquakes within each zone are specified using historical data and a Gutenberg-Richter (G-R) relationship that relates earthquake magnitude to number of occurrences. Specific characteristics (e.g., location or epicenter, fault motion, hypocentral depth, fault length) of each earthquake are defined using known faults and fault models, previously derived source regions, and geophysical knowledge. For each earthquake in the stochastic catalog, estimates of local soil conditions and ground motion prediction equations are used to determine peak ground acceleration (PGA) at each grid point. The estimates of local soil conditions are based on tectonic regime and topographic slope following *Allen and Wald* [2007].

Earthquake risk is presented in terms of affected population and affected GDP for areas that experience ground motion with an intensity consistent with modified Mercalli intensity (MMI) equal to VI or greater. Ground motion at MMI VI may cause moderate damage to poorly built structures, and slight damage such as cracks in most average structures. It will be felt by almost everyone. Semi-empirical vulnerability functions are used to estimate MMI from PGA following *Daniell* [2014].

Table 4. Climate Models Used With the GLOFRIS Model

Climate Model	Description
GFDL ESM2M	GFDL Earth System Model 2 with medium resolution
HadGEM2-ES	Hadley Global Environment Model 2—Earth System
MIROC-ESM-CHEM	MIROC (Model for Interdisciplinary Research on Climate) Earth System CHASER-coupled Model (Atmospheric Chemistry version)
IPSL-CM5A	Institut Pierre Simon Laplace Coupled Model 5
NorESM1-M	Norwegian Earth System Model with medium resolution

Earthquake risk is also presented in terms of fatalities and capital losses using vulnerability functions as described by *Daniell* [2014] and calibrated using *Daniell et al*. [2011]. The fatality and capital loss vulnerability functions are empirically derived using past ground motion event data versus capital stock. The building vulnerability is brought in via the averaging of the various vulnerability functions for building types for each country. As such, capital loss estimates are only applicable for province-level assessment as the average vulnerability functions apply to both the urban and rural regions of a country, despite the fact that capital values (or replacement costs) will differ between urban and rural areas. Thus, there is likely a slight overestimation of loss in countries with a large difference between earthquake vulnerability in urban (less vulnerable structures) and rural (more vulnerable structures) areas. However, the extent of the difference varies by country. Checks against other vulnerability functions of authors were also made, and the vulnerability functions were adjusted to be consistent with these other functions where there was not enough data to support a significant difference.

2.2. Flood Model

The flood model uses several modules of the Global Flood Risk with IMAGE Scenarios (GLOFRIS) global flood risk-modeling cascade. The first step is the simulation of daily discharge at a horizontal resolution of 0.5° × 0.5° using the PCRaster Global Water Balance (PCR-GLOBWB) global hydrological model [*Beek and Bierkens*, 2008; *Beek et al*., 2011]. For present-day climate, the model boundary conditions were daily meteorological data at 0.5° × 0.5° resolution. These data are derived from analysis of data for the years 1960–1999 and are provided by the EU WATCH project [*Weedon et al*., 2010].

The second step in the hazard modeling is the simulation of daily within-bank and overbank flood volumes, again at a spatial resolution of 0.5° × 0.5°. This is carried out using the PCR-GLOBWB extension for dynamic routing, DynRout (PCR-GLOBWB-DynRout), which simulates flood-wave propagation within the channel as well as overbank [*Ward et al*., 2013; *Winsemius et al*., 2013].

From this daily time series of flood volumes, estimates of flood volumes per grid cell (0.5° × 0.5°) were derived for selected return periods (2, 5, 10, 25, 50, 100, 250, 500, and 1000 years). The return period estimates are derived using extreme value statistics based on the Gumbel distribution and the daily nonzero flood volume time series derived from the hydrological model. These flood volumes were then used as input to the GLOFRIS downscaling module to calculate flood depths at a resolution of 30′′ × 30′′ [*Winsemius et al*., 2013].

The GDP and population affected by floods for each return period were based on the population or GDP in each grid cell that had flood depths greater than 10 cm at the selected return periods. The average annual values at each grid point were derived by integrating over the nine return-period loss estimates. The annual average and return period values for GDP and population affected by floods were determined by summing the losses within each Level 1 (the first subnational level, e.g., a state in the United States or a province in Canada) administrative region and within each country.

To estimate flooding in 2030 and 2080, the same methodology as described above is used except that the GLOFRIS model boundary conditions were future daily data from five climate models (Table 4). The five climate models used the two RCPs shown in Table 3. The climate data used were previously bias corrected by *Hempel et al*. [2013], using the 1960–1999 EU WATCH data as the baseline. Unless explicitly stated otherwise, the flood risk for 2030 and 2080 is the average of the five GCM estimates.

2.3. Exposure Data

A multistep correction process was used to generate the spatial distribution of estimated 2015 GDP. First, national-level data were adjusted to 2015 using the CATDAT database [*Daniell et al*., 2012]. The national-level 2015 GDP values were then adjusted to match the individual province-level GDP per capita data derived from provincial and municipal government and World Bank estimates. Finally, each province-level region had separate values of GDP per capita, and GDP was distributed spatially throughout the region as a function of 1-km resolution population data.

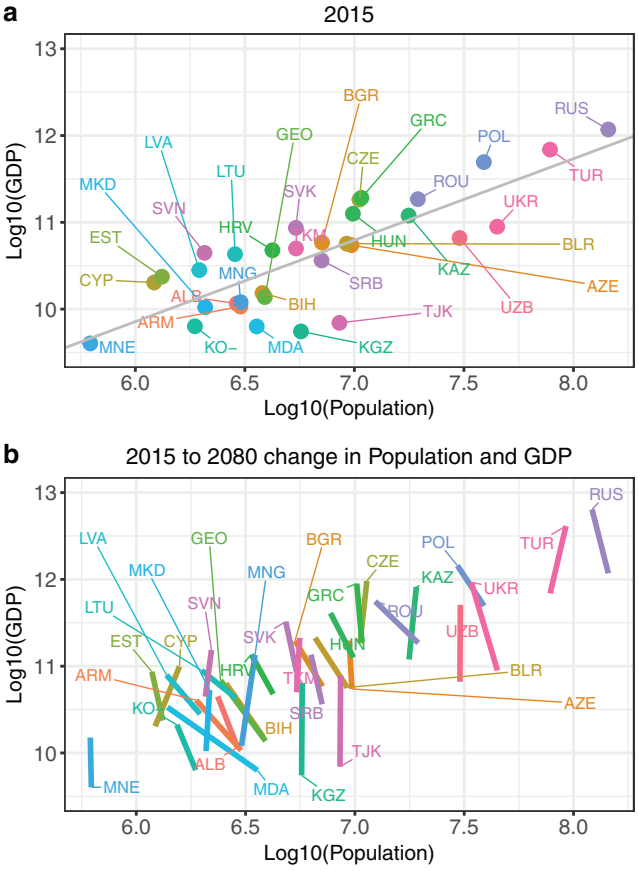

Figure 1. Log–log plot of population versus GDP for the ECA countries. Each country is identified by its ISO Alpha-3 country code. (a) National-level GDP ($) and population estimates are for 2015. The light gray line is a linear least squares fit to the data. The correlation between GDP and population is 0.95. (b) The evolution of GDP and population from 2015 to 2080 (thick lines). The bottom of each line represents the population and GDP in 2015. The top end of each line represents the 2080 average GDP and population of the five SSPs. Thin lines are used for labeling. The colors are intended to make it easier to distinguish individual countries.

The 2010 population estimates were projected to 2015 values at a Level 1 administrative (province) level using the 2010 round of census data and census growth rates for each of the 863 province level units. The 2010 province level data were updated to 2015 using growth rates determined from the 2000 and 2010 census round data and other subnational-level demographic survey data sets within CATDAT [*Daniell et al*., 2011]. In most cases, growth rates were determined from the 2000 and 2010 census surveys.

Future exposure data (GDP and population) for 2030 and 2080 were developed using the Integrated Model to Assess the Global Environment (IMAGE) model of PBL Netherlands Environmental Assessment Agency [*Bouwman et al*., 2006; *van Vuuren et al*., 2007], and socioeconomic conditions associated with the SSPs in Table 2.

While the 2015 population and GDP data are relatively robust, the projections to 2030 and 2080 should be considered as scenarios. The spread in the GDP and population values for the five SSPs is greater in 2080 than in 2030. For more information on future population scenarios see *Samir and Lutz* [2017]. For more information on future GDP scenarios see *Dellink et al*. [2017].

A summary of the estimated population and GDP for countries in the ECA region is shown in Figure 1. National population and GDP for 2015 in the ECA region differ by more than two orders of magnitude among countries (Figure 1a), and there is a high level of correlation (0.95) between a country's population and GDP. The top two countries for population and GDP are the Russian Federation (RUS) and Turkey (TUR). Montenegro (MNE) has the smallest population and GDP. The mean of GDP from the five SSPs for all countries will be greater in 2080 than in 2015, in some cases by over an order of magnitude (Figure 1b). While mean GDP increases for all countries, there is more variability in future population growth. For some countries in the ECA region the 2080 mean of population from the five SSPs will be less than the 2015 population. For example, for two of the three countries with the largest population in the ECA region, the Russian Federation and Ukraine (UKR), the 2080 mean of population from the five SSPs is less than the 2015 population.

3. Results

3.1. Current Risk

3.1.1. National-Level Risk

A summary at the national level of the average annual population and GDP affected by earthquakes and flooding is shown in Figure 2. Of all the countries in this study, Turkey (TUR) has the greatest annual average population (more than 1 million) and GDP (more than $10 billion) affected by earthquakes with Uzbekistan (UZB) having the second greatest population and Romania (ROU) the second greatest GDP (Figures 2a and 2b). Turkey's exposure is due in large part to the concentration of Turkey's urban population along the Anatolian fault and its large economy. The country with the greatest annual average population (2 million) and GDP ($20 billion) affected by flooding is the Russian Federation (RUS).

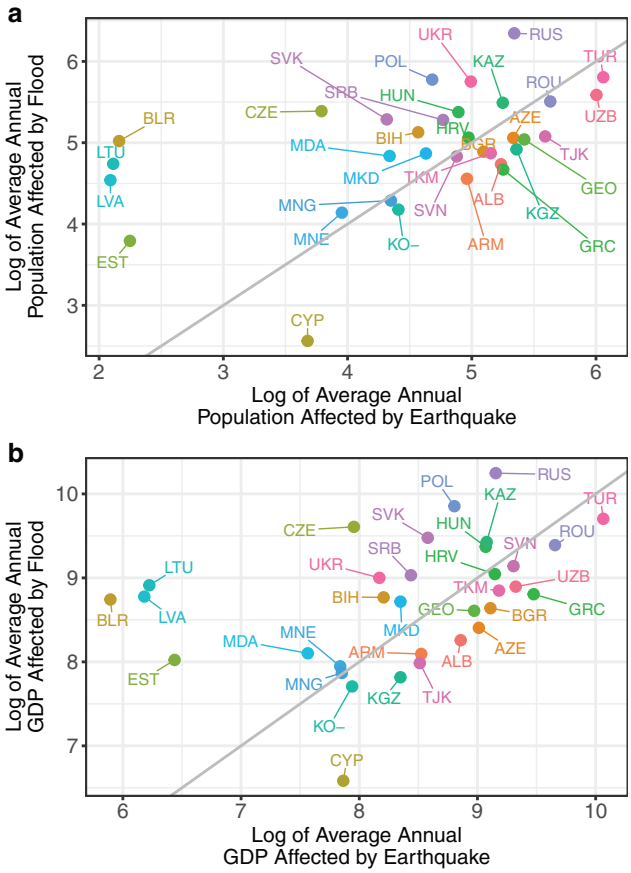

Figure 2. Risk of earthquakes and floods in 2015 in terms of (a) the average annual affected population and (b) GDP ($) for all nations in the study. The abbreviations are based on ISO Alpha-3 notation. Note that all values are plotted on a log10 scales. The gray line shows the 1:1 relationship between the annual average affected by floods and earthquakes. The similarity between the GDP and population results is due to the large correlation between a country's GDP and population. The colors are intended to make it easier to distinguish individual countries.

A different view of risk is seen when assessing annual average risk relative to the total national population or GDP rather than absolute population or GDP (Figure 3). In relative terms, Georgia (GEO) and Albania (ALB) are the countries whose populations and GDP have the greatest annual average chance of being affected by earthquakes (~6%–7%). This is consistent with large events in the past such as 1991 and 2002 in Georgia and the early 1900s (1905, 1930) in Albania [*National Geophysical Data Center/World Data Service (NGDC/WDS)*, 2017]. The country with the greatest annual average risk in terms of population being affected by floods, in relative terms, is the Slovak Republic (SVK, ~4%), followed closely by Bosnia and Herzegovina (BIH) and FYR Macedonia (MKD), and the country with the greatest annual average risk in terms of GDP being affected by floods is the FYR Macedonia (~5%).

A spatial representation of the annual average population at risk of earthquakes and floods in 2015 is shown in Figure 4. Essentially the same pattern would be seen with GDP because of the high correlation between a country's population and GDP. The Russian Federation (RUS) is the largest country in the study area, and has the largest GDP, population and annual average risk of floods in terms of affected people and GDP (Figures 2 and 4). Turkey (TUR), Uzbekistan (UZB), Romania (ROU), and Tajikistan (TJK) are at a greater risk of earthquakes than the Russian Federation (Figures 2a and 4).

The loss exceedance probabilities that contribute to the GDP and population annually affected by earthquakes and floods vary by country. A heat map can provide a qualitative sense of how risk varies among countries and perils in both absolute and relative terms (Figure 5). The absolute and relative flood risk tends to be fairly constant for all the return periods displayed in Figure 5 whereas the earthquake risk tends

to increase with longer return periods. This is consistent with the more frequent nature of flood events relative to damaging earthquakes; however, it may also be related to some of the assumptions, mentioned in the discussion, that were made when modeling flood risk. Specifically, the flood modeling assumes that there are no flood defenses and that 100% of population or GDP in a grid cell is affected in any cell with any inundation depth.

The earthquake model also estimated fatalities and capital losses. The distribution of fatalities versus affected population, and capital loss versus GDP, for the 250-year return period is shown in Figure 6. There is a weak correlation between affected population and fatalities and between affected GDP and capital loss. However, it appears that countries in the European Union and Turkey tend to have a lower capital loss to affected GDP ratio than non-European Union countries. Note that the ranking of countries by population or GDP affected by the 250-year return period earthquake is not the same as that for the annual average (Figure 2) because of differences in their probabilities of loss (Figure 5).

3.1.2. Province-Level Risk

Province-level results for Turkey (Figure 7) and Ukraine (Figure 8) are presented as two examples of how earthquake and flood risk, and population and GDP, vary within a country. For Turkey, in absolute and relative terms, the province with the greatest population at risk of flooding is in south-central Turkey (Figures 7a and 7c). For earthquake risk, the province with the highest relative earthquake risk (Figure 7b) is in the southwest and the province with the highest absolute earthquake risk (Figure 7d) is in the northwest. The highest absolute earthquake risk corresponds with the province with the highest population (Figure 7e) and GDP (Figure 7d), but the highest absolute flood risk occurs in a province without an extreme in GDP or population.

For Ukraine, in absolute and relative terms, the province with the greatest population at risk of flooding is in northeast province (Figures 8a and 8c). In contrast to Turkey, the flood risk in Ukraine is distributed more evenly across the country. Earthquake risk in Ukraine is concentrated in the southern provinces of the country (Figures 8b and 8d). The province with the highest GDP and population in Ukraine is in the north central part of the country (Figures 8e and 8f). The provinces with the greatest risk differ from the provinces with high GDP and population.

3.2. Future Changes in Risk

There is a significant amount of intercountry variability in the future change in the risk of earthquakes and floods affecting a country's population and GDP. The results shown in Figures 9 and 10 for population, GDP, and population affected by earthquakes are based on the difference between the average of five results for 2080 and the results for 2015. The results shown in Figures 9 and 10 for GDP and population affected by floods are based on the difference between the average of 15 results for 2080 and the results for 2015. Consistent with Figure 1b all countries experience an increase in GDP (Figure 9e) but some countries see a decrease in population (Figure 9f).

We show average results for the 2080–2015 differences in population, GDP, and earthquake- and flood-affected population (Figure 9) and GDP (Figure 10) to focus on the general trends in the results. The individual SSPs are unlikely to represent exactly what will happen in the future; instead, they represent a wide range of possibilities that could well span what will happen (Table 2). In fact, five different countries could follow five different SSPs. In addition, there is uncertainty in the results produced using the flood and earthquake risk models and variability among the climate models used with the flood risk model. Thus, in a manner analogous to ensemble forecasting where the ensemble mean has the lowest root-mean-square error [*Park et al*., 2008], for earthquake risk we choose to examine the mean of the earthquake risk consistent with the five SSPs and for flood risk we choose to examine the mean of the 15 views of flood risk consistent with the five climate models (Table 4) combined with the three combinations of SSPs and RCPs (Table 3) for flood risk.

The percentage change in relative risk of a country's population being affected by floods (Figure 9a) depends to a small extent on the change in population (Figure 9f). Similarly, the change in absolute risk of a country's population being affected by floods (Figure 9c) depends to a small extent on the projected change in population. In contrast to floods, the percentage change in the relative risk of a country's population being affected by earthquakes (Figure 9b) depends to a great extent on the change in population

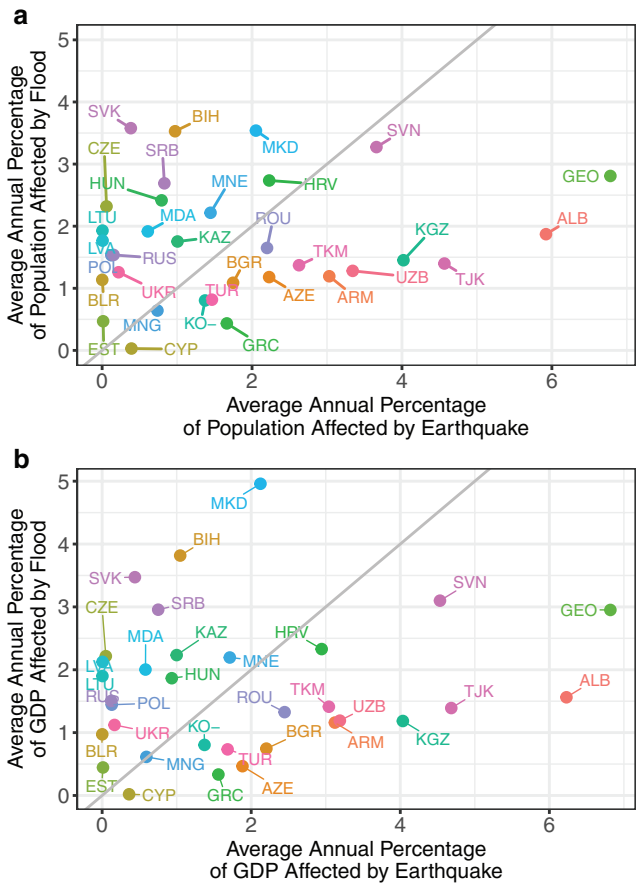

Figure 3. Risk of earthquakes and floods for 2015 in terms of the average annual percentage of (a) affected population and (b) GDP ($) for all nations in the study. The abbreviations are based on ISO Alpha-3 notation. The gray line shows the 1:1 relationship between the annual average affected by floods and earthquakes. The similarity between the GDP and population results is due to the large correlation between a country's GDP and population. The colors are intended to make it easier to distinguish individual countries.

(Figure 9e). Similarly, the change in absolute risk of a country's population being affected by earthquakes (Figure 9d) depends to a modest extent on the projected change in population.

The change in relative risk of a country's GDP being affected by floods (Figure 10a) depends to a small extent on the change in GDP (Figure 9e). Similarly, the change in absolute risk of a country's GDP being affected by floods (Figure 10c) depends to a small extent on the projected change in GDP. The change in the relative and absolute risk of a country's GDP being affected by earthquakes (Figures 10b and 10d) depends to a small extent on the change in GDP. However, the percentage change in relative risk of a country's population being affected by earthquakes (Figure 9b) is controlled to a great extent by the relative change in the country's population (Figure 10f). Also, the percentage change in relative risk of a country's GDP being affected by earthquakes (Figure 10b) is controlled to a great extent by the relative change in a country's GDP (Figure 10e).

Within a country, the population and GDP affected by earthquakes will also change in response to an increase or decrease in a country's GDP and population. Turkey, a country where population is expected to increase (Figure 11a), and Ukraine, a country where population is expected to decrease (Figure 11b), are used to illustrate such changes. The black line in Figure 11 represents the mean value of the earthquake risk results from the five SSPs. The range between the maximum and minimum populations derived from the five SSPs (Table 2) grows significantly from 2030 to 2080 and is consistent with growing uncertainties in results between 2030 and 2080. The results in Figure 11 show that the change in populations associated with the different SSPs can have a dramatic impact on the annual average population at risk of being affected by earthquakes in 2030 and 2080. Similar results are obtained when looking at changes in GDP and affected GDP.

Two RCPs and two SSPs are used to illustrate the contributions of future changes in climate and population on Turkey's and Ukraine's flood risk in 2030 and 2080 (Figure 12). Three sets of model runs were completed to assess the relative roles of changes in climate and changes in population. One set can be used to examine the influence of changes in climate by fixing population at 2015 values and using the results from five climate models responding to two different RCPs as boundary conditions for the flood model. Another set can be used to examine the influence of changes in population using current atmospheric conditions and having population follow two different SSP pathways. The third set can be used to examine the combined impact of changes in climate and population using three combinations of SSPs and RCPs. A similar exercise was done using GDP as exposure but is not shown.

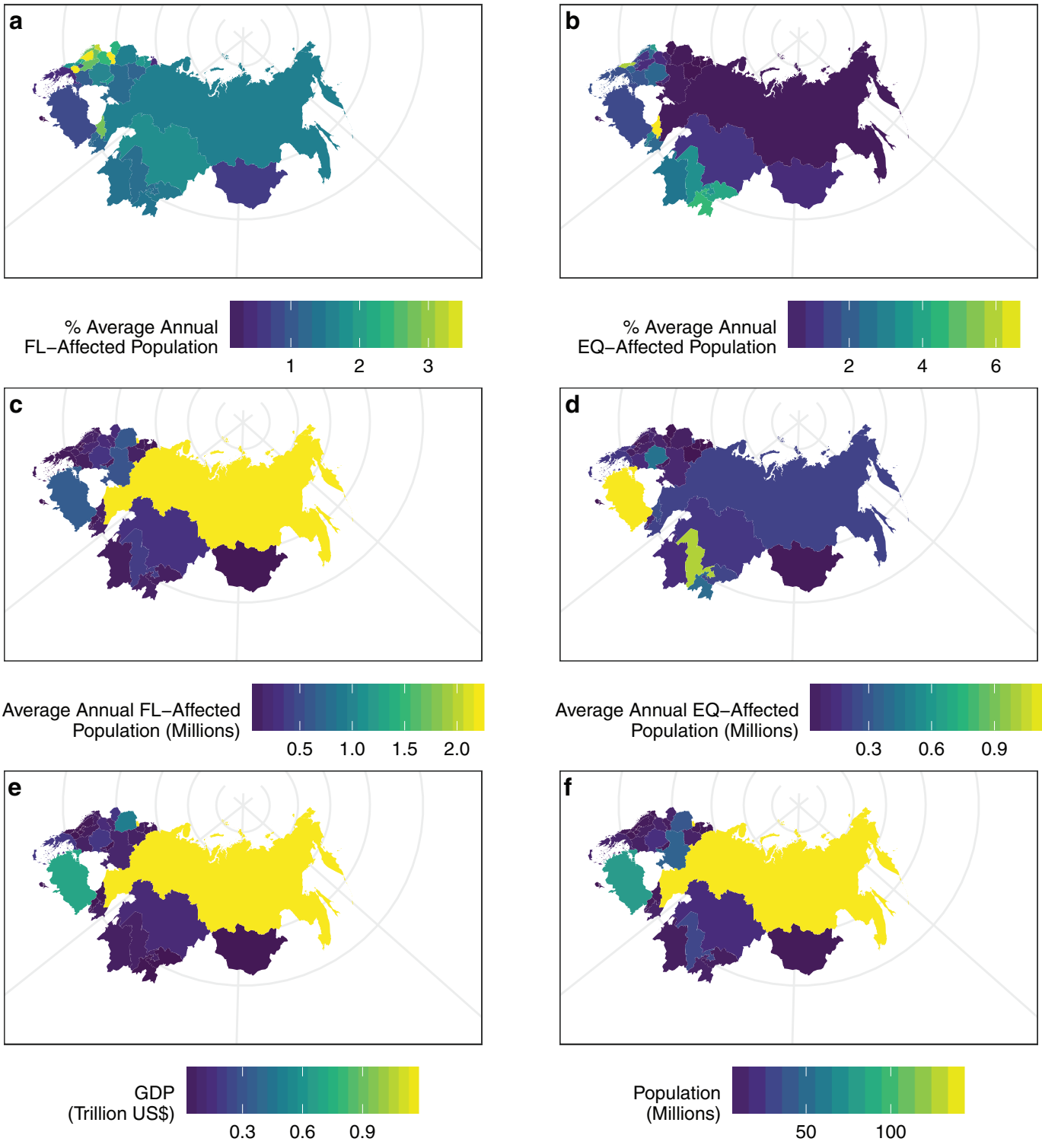

Figure 4. Spatial distribution by country of 2015 average annual percent of population affected by (a) flood and (b) earthquake, the average annual population affected by (c) flood and (d) earthquake, and the national level of (e) GDP and (f) population. Similar patterns would be seen if GDP were displayed instead of population. The longitude lines are 50°, 100°, and 150° east. Latitude lines range from 90° (where longitude lines cross) to 40° (the outer circle on the maps) north in 10° increments. Flood is abbreviated as FL and earthquake as EQ.

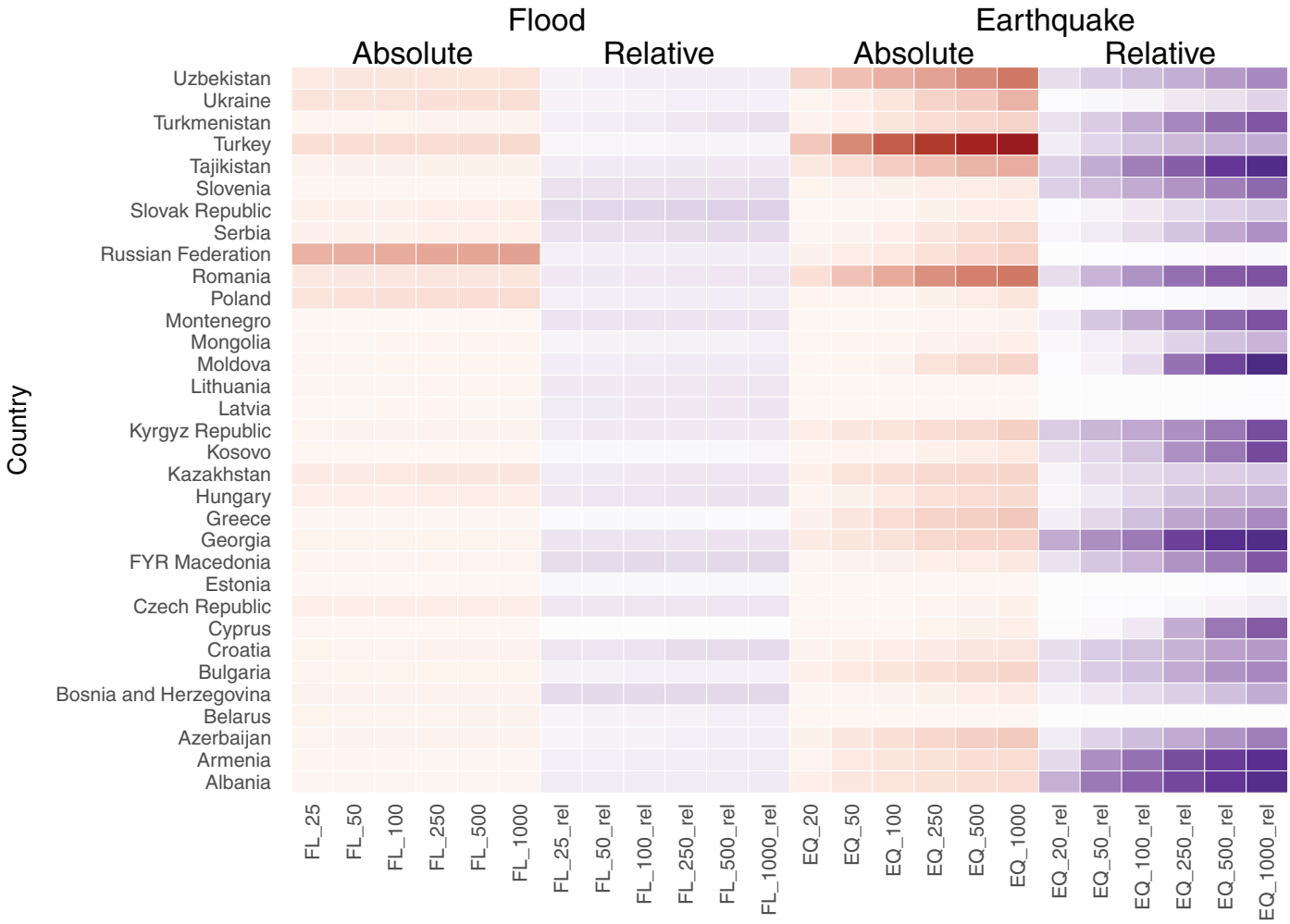

Figure 5. Heat map showing relative values for population affected by floods (left half) and earthquakes (right half) at return periods of 25, 50, 100, 250, 500, and 1000 years. The red colors represent affected population in absolute terms, the purple colors represent population in relative terms. The intensity for each color is scaled over the values for both perils: The darkest and lightest color occurs in the column where with the largest and smallest affected population value, respectively. Thus the largest value for affected population occurs for the 1000-year return period for earthquakes in Turkey and the largest value for the affected population in relative terms occurs for the 1000-year return period for earthquakes in Georgia. The return period patterns for GDP are very similar and not shown. Flood is abbreviated as FL and earthquake as EQ.

For Turkey (Figure 12a), the mean flood-affected population associated with the five GCMs slightly decreases or remains almost constant, between 2015 and 2080 for each SSP and RCP combination (top row of Figure 12b). However, the spread in results from the climate models suggest the flood-affected population might either increase, decrease, or remain the same depending on the SSP, RCP, and GCM combination. For Ukraine (Figure 12b), the mean flood-affected population associated with the five GCMs decreases between 2015 and 2080 for each SSP and RCP combination (top row of Figure 12b). This observation also holds for each GCM run. The spread of 2080 model results for Turkey is greater than that for Ukraine suggesting that the results for Ukraine may be more robust than those for Turkey. However, it would be difficult to confirm this without more analysis.

Model runs that isolate the impact of changes in climate and population can be used to compare their relative roles in changing the combined flood risk (Figure 12). With a fixed population the mean results from the five GCMs using two RCPs suggest that climate change would result in a decrease in the annual average flood-affected populations in Turkey and Ukraine. However, with a fixed climate, changes in population consistent with the two SSPs suggest that the population growth in Turkey increases the population affected by flood whereas population decline in Ukraine decreases the population affected by flood. For Turkey, the spread in combined model results (top row of Figure 12a) is associated with the relatively wide

range in flood risk produced by changes in climate as well as the relatively large population differences between SSP2 and SSP3. For Ukraine, the spread in combined model results (top row of Figure 12b) is dominated by the differences in climate model runs as the two SSPs have relatively similar population pathways.

4. Discussion

This study analyzes the relative role of future changes in climate and socioeconomic factors on earthquake and flood risk in ECA countries. For the GDP and population exposure in the ECA region, the SSPs suggest an overall increase in GDP for all countries whereas the population increases or decreases depending on the country (Figure 1b). Flood hazard estimates change in response to different RCPs used with the five climate models, whereas earthquake hazard is assumed to be constant. Vulnerability functions (for fatalities and capital loss from earthquakes) and affected exposure functions (for population and GDP) are constant across a single country or province, but differ between countries.

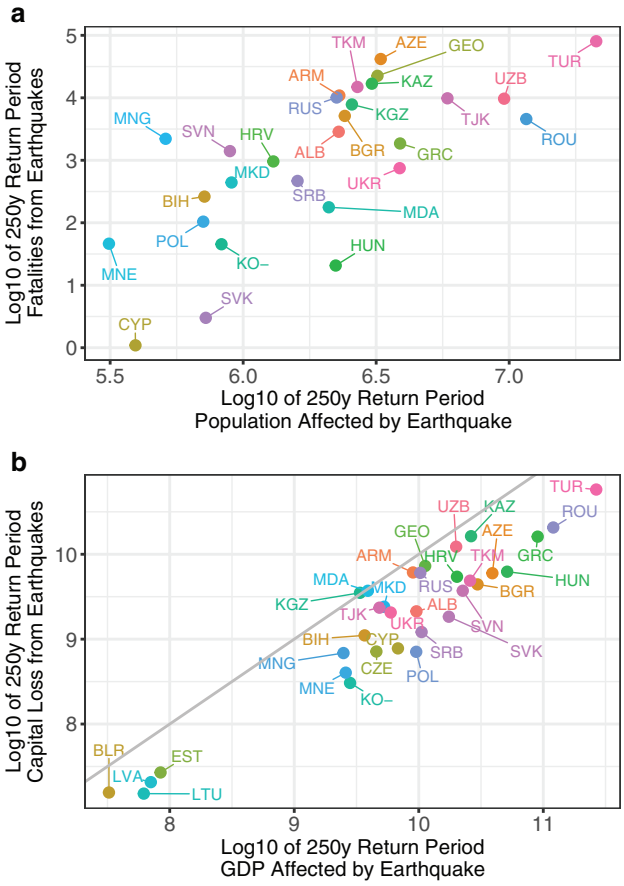

Figure 6. Distribution of 250-year return period impacts. (a) The log10 of fatalities as a function of population affected by 250-year return period earthquakes. (b) Capital loss ($) as a function of GDP affected by 250-year return period earthquakes. The gray line shows the 1:1 relationship between the annual average affected by floods and earthquakes. The colors are intended to make it easier to distinguish individual countries.

There is a linear relationship between the relative change in earthquake risk and the relative change in population and GDP (Figure 13). Here, relative change is defined as the difference between 2080 and 2015 values divided by 2015 values. The linearity is a result of the assumption of the hazard and vulnerability being constant over time, no migration of exposure, and the national-level multipliers for future population and GDP scenarios.

The relative change in flood risk (Figure 14) is more complex than that for earthquake (Figure 13) due to the spatial variation in future flood hazard driving departures from a 1:1 relationship with the relative change in exposure. Changes in atmospheric radiative properties as specified by the RCPs change flood location, intensity and frequency in the GCMs, and thereby the flood hazard. The vertical distance from the 1:1 relationship between relative change in population or GDP and the relative change in flood risk can be used to qualitatively assess the countries' susceptibility to changes in flood hazard induced by climate change. The countries with the largest amount of climate change-induced flood risk are those that lay farthest vertically from the 1:1 line in Figure 14.

One can define six regions (see the roman numerals in Figure 14a) to qualitatively assess the relative role of climate change and change in population (or GDP) on the relative change in flood-affected population (or GDP). The different regions are defined by the dashed and solid lines in Figure 14.

1. Region I is where the relative increase in flood-affected population (or GDP) is driven by an increase in population (or GDP) and by a climate change-induced increase in flooding.

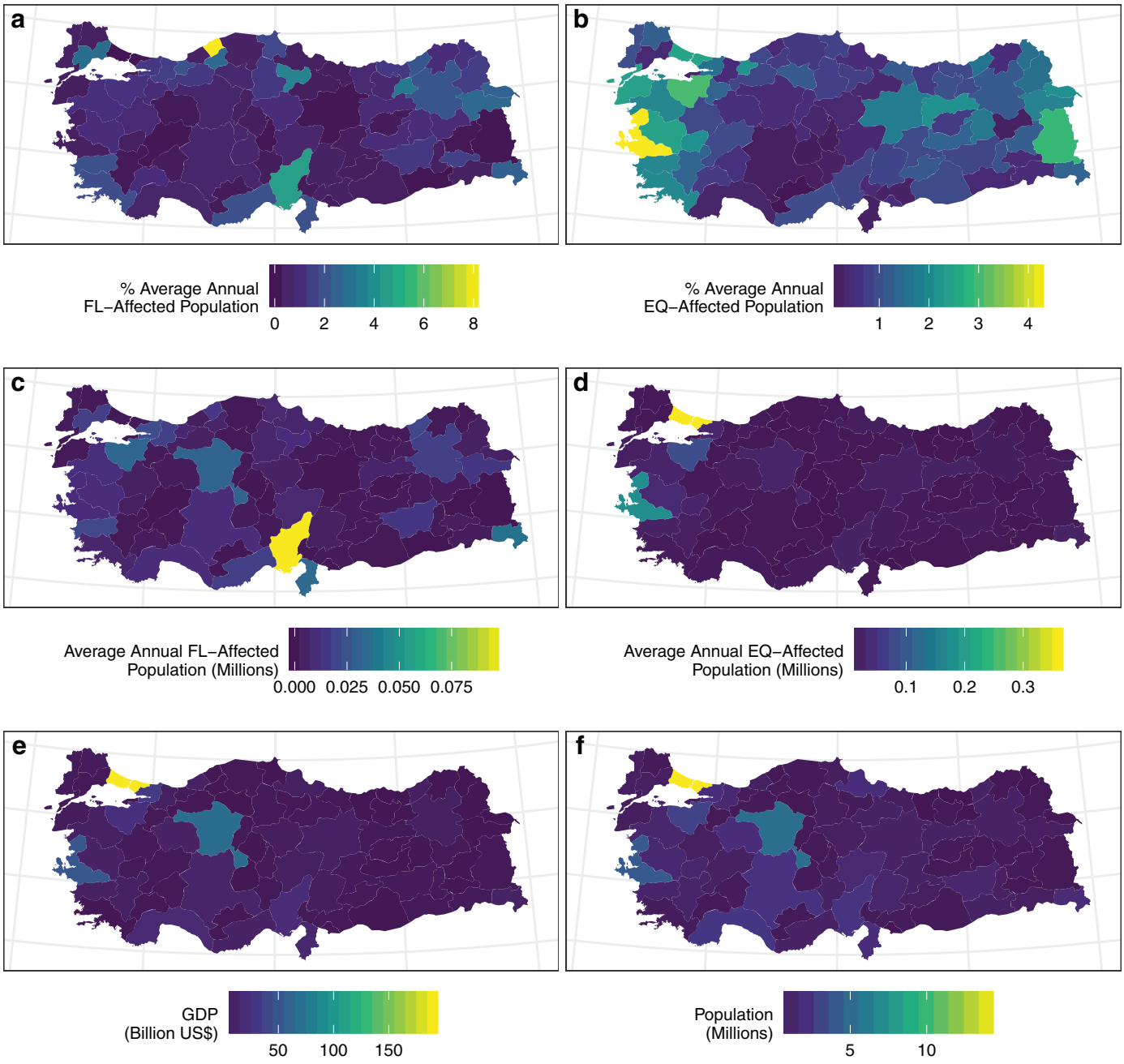

Figure 7. Province-level results for Turkey. (a) Average annual percentage of the population affected by flood. (b) Average annual percentage of population affected by earthquake. (c) Average annual population affected by flood. (d) Average annual population affected by earthquake. (e) GDP. (f) Population. Longitude lines denote 25°E–45°E in increments of 5°. Latitude lines range from 36°N to 42°N in increments of 2°. Flood is abbreviated as FL and earthquake as EQ.

2. Region II is where an increase in population (or GDP) would cause an increase in flood-affected population (or GDP), but this increase would be tempered by a climate change-induced decrease in flooding.
3. Region III is where a climate change-induced decrease in flooding is so large that it overwhelms the relative increase in population (or GDP).
4. Region IV is where a relative decrease in flood-affected population is driven by both a decrease in population and by a decrease in climate change-induced flooding.

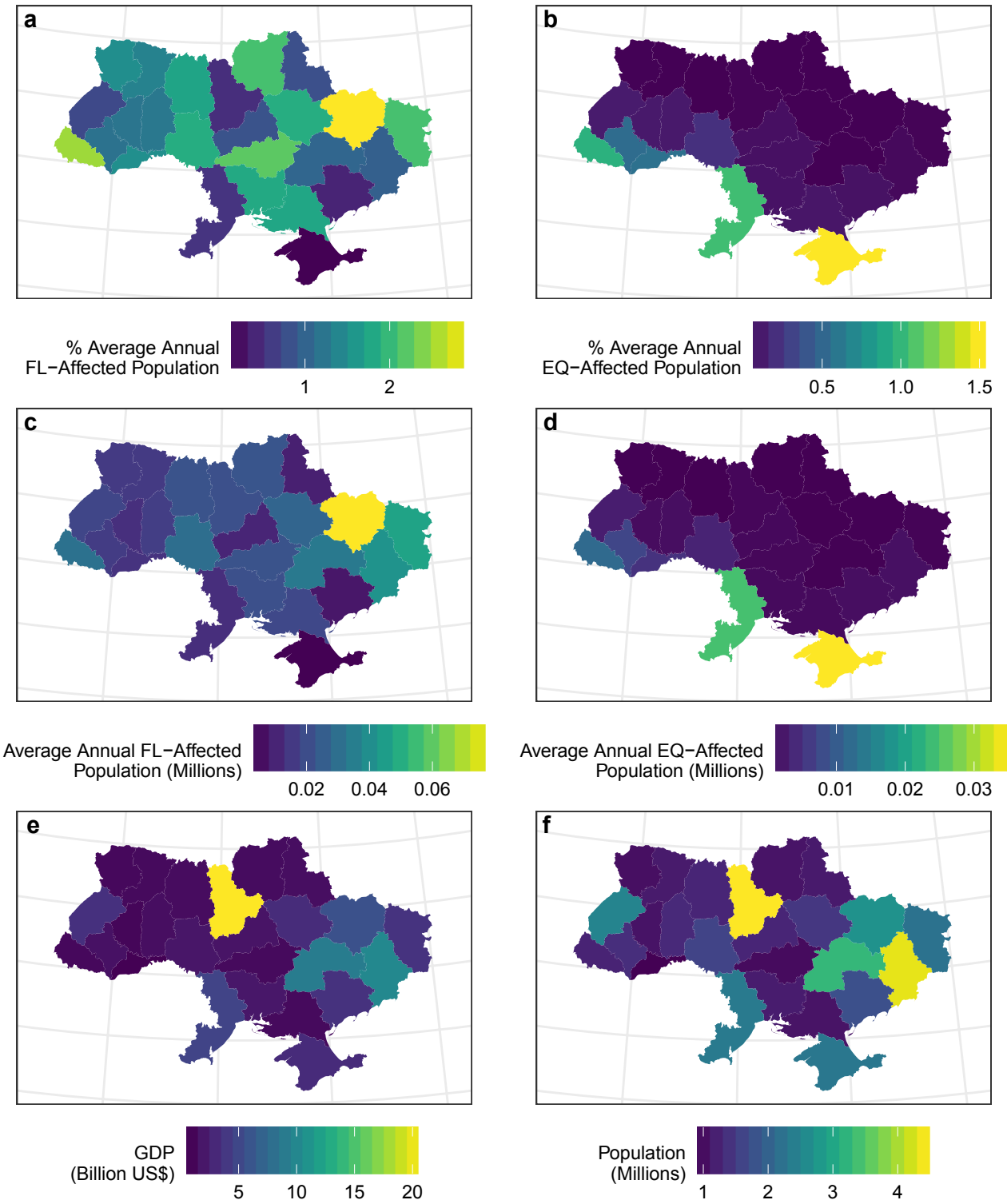

Figure 8. Province-level results for Ukraine. (a) Average annual percentage of the population affected by flood. (b) Average annual percentage of population affected by earthquake. (c) Average annual population affected by flood. (d) Average annual population affected by earthquake. (e) GDP. (f) Population. Longitude lines denote 25°E–40°E in increments of 5°. Latitude lines range from 44°N to 52°N in increments of 2°. Flood is abbreviated as FL and earthquake as EQ.

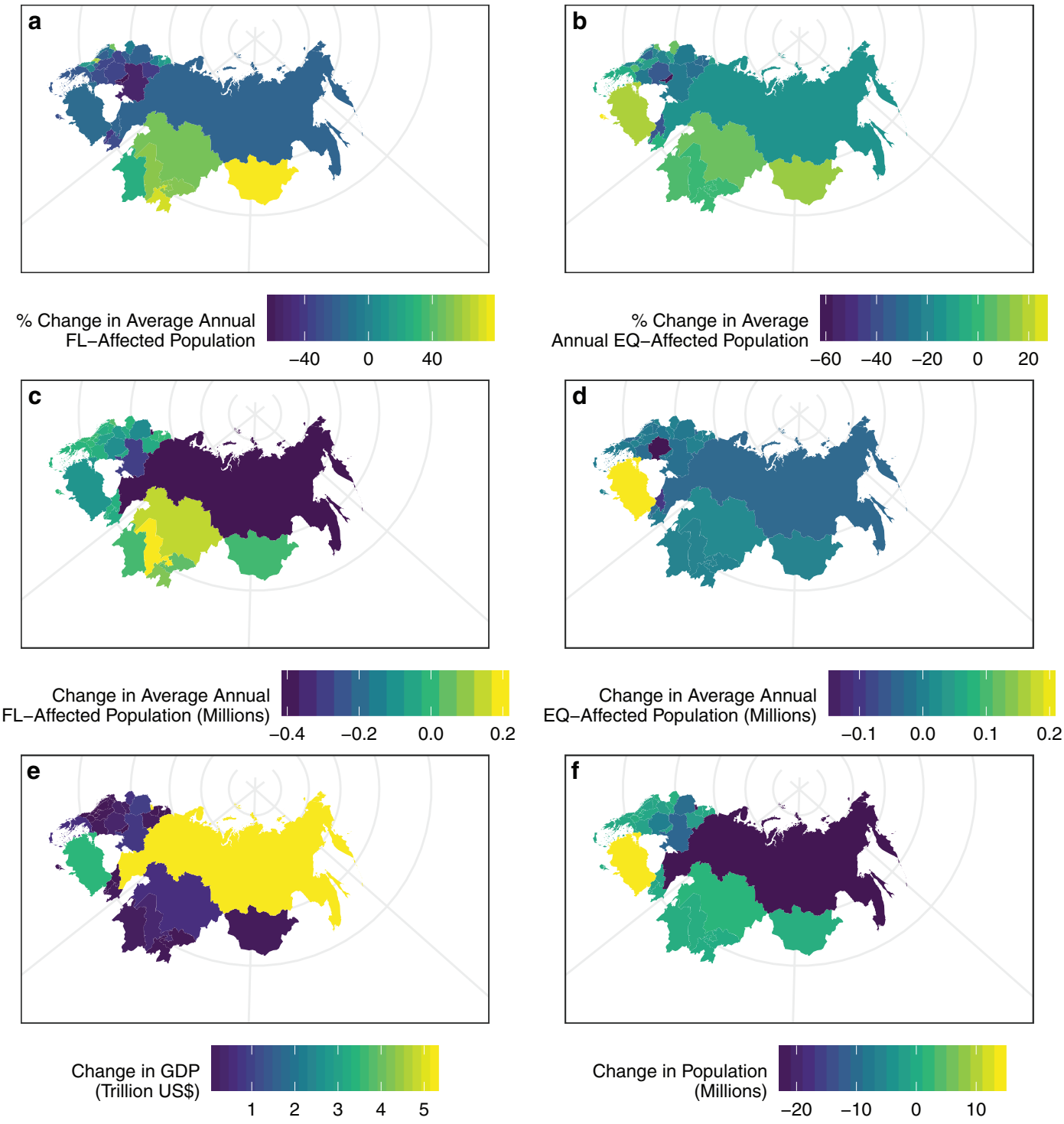

Figure 9. Spatial distribution by country of the change in: average annual percent of population affected by (a) flood and (b) earthquake, the average annual population affected by (c) flood and (d) earthquake, and the national level of (e) GDP, and (f) population. The national-level change in average annual percent (a and b) equals $100*(2080_X - 2015_X)/2015_X$, where X is affected population. The change in average annual affected population, GDP and population equals $(2080_Y - 2015_Y)$, where Y is annual affected population, GDP, or population. The longitude lines are 50°, 100° and 150°E. Latitude lines range from 90° (where longitude lines cross) to 40° (the outer circle on the maps) north in 10° increments. Flood is abbreviated as FL and earthquake as EQ.

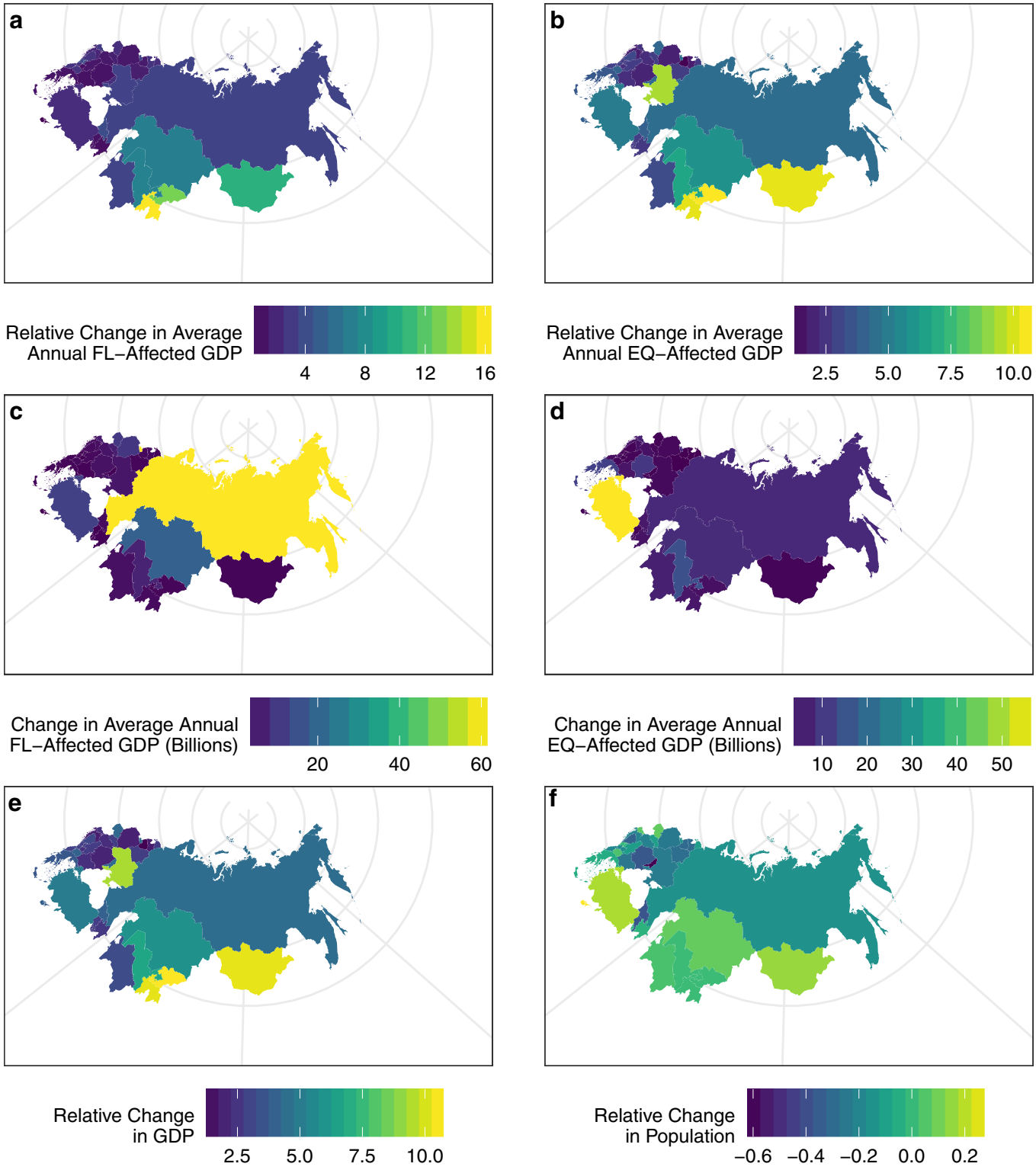

Figure 10. Spatial distribution by country of the change in: average annual percent of GDP affected by (a) flood and (b) earthquake, the average annual GDP affected by (c) flood and (d) earthquake, and the relative change in national (e) GDP and (f) population. The national-level change in average annual affected GDP (a and b), and the relative change in GDP and population (e and f) equals $(2080_X - 2015_X)/2015_X$, where X is affected GDP, GDP, or population. The change in average annual affected GDP (c and d) equals $(2080_Y - 2015_Y)$, where Y is affected GDP. The longitude lines are 50°, 100°, and 150°E. Latitude lines range from 90° (where longitude lines cross) to 40° (the outer circle on the maps) north in 10° increments. Flood is abbreviated as FL and earthquake as EQ.

5. Region V is where the relative decrease in flood-affected population due to a lower population is countered by a climate change-induced increase in flooding.
6. Region VI is where a climate change-induced increase in flooding so large that it overwhelms the decrease in risk due to a decrease in population.

For example, despite having little relative change in population, Tajikistan (TJK) experiences one of the largest relative increases in populations affected by flooding because of climate change (Figure 14a). In contrast, for Cyprus (CYP), climate change effects temper the relative increase in flood-affected population that would be expected purely based on the large increase in relative population (Figure 14a). For Tajikistan, climate change has the largest increasing effect on relative flood-affected GDP, and for Ukraine (UKR) climate change has the largest decreasing effect on relative flood-affected GDP (Figure 14b). Finally, some countries, such as Romania (ROU), fall near to the 1:1 line and experience relative changes in flood risk that are related mainly to changes in exposure, and climate change impacts on their flood risk are expected to be marginal.

The view of relative change in flood risk can inform efforts to prioritize climate change adaptation efforts related to managing flood risk. As an example consider that the model scenarios suggest that Turkey (TUR) (Region III) and Georgia (GEO) (Region V) will see a similar decrease in relative flood-affected population (Figure 14a). The decrease in Turkey occurs despite the increase in population whereas the decrease in Georgia is less than expected based on its projected change in population. Thus, a first-order approximation would imply that there might be more value in projects that reduce flood risk in Georgia than for those in Turkey given that climate change-related flood risk is expected to increase in Georgia but decrease in Turkey. Regardless of the choice of country, improved modeling would be needed to make a robust decision regarding risk management within a specific country. This would include, for example, more specific information on the location of exposure, the incorporation of flood defenses in the flood models and the use of vulnerability functions that are more appropriate for a specific project, to produce more sophisticated modeling results for projects of interest. In addition, other factors beyond technical considerations need to be considered [*Murnane et al.*, 2016], including the capacity of the country to manage a project and the interest within the country in the disaster risk management project.

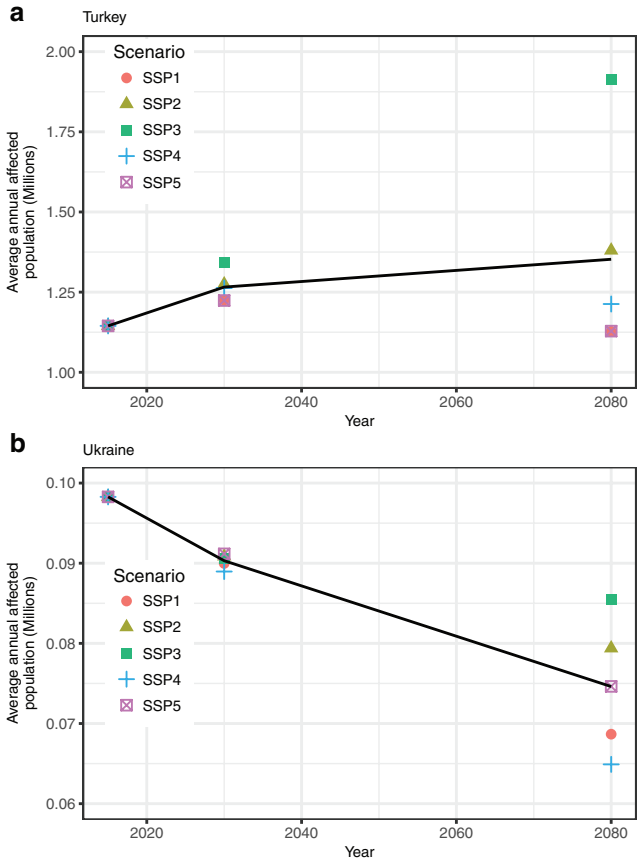

Figure 11. Average annual population affected by earthquakes in Turkey (top) and Ukraine (bottom) for three time slices: 2015, 2030, and 2080. The black line in A and B shows the mean value based on the population derived from the five SSPs. The earthquake hazard is constant for the three time slices so the change in population drives the change in affected population.

The results from the risk assessment will be used to focus the attention of national-level decision makers on areas with high flood and earthquake risk and to support the prioritization of studies to further quantify risk. However, these results provide only a preliminary view of risk and should not be used for the design of risk reduction measures such as flood protection, retrofitting of buildings or risk-informed urban planning. Such measures require more detailed and calibrated models that include critical information on local conditions

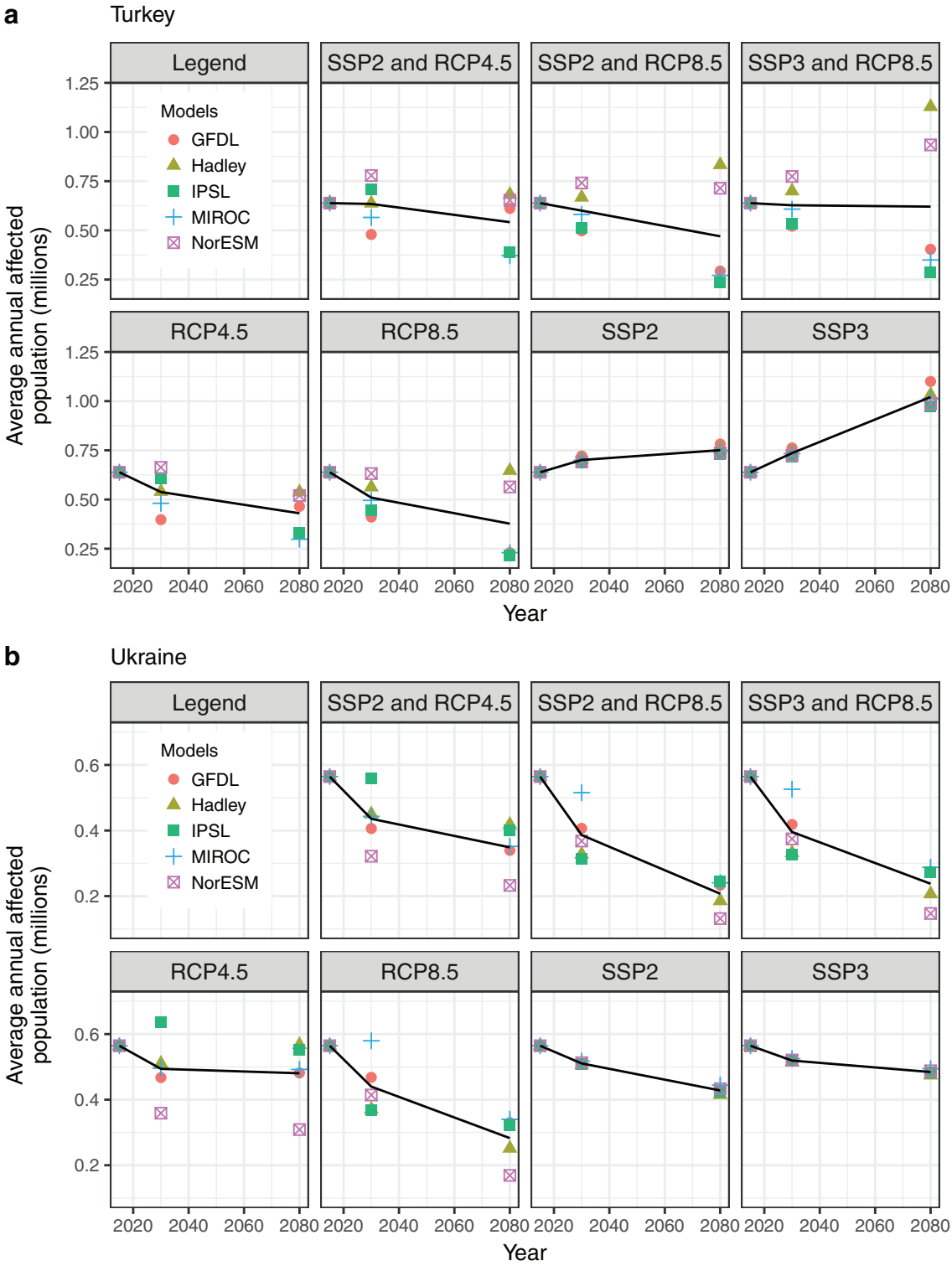

Figure 12. Average annual population affected by floods in Turkey (a) and Ukraine (b) for three time slices: 2015, 2030, and 2080. The black lines in a and b show the mean value for affected population derived from the five GCMs with the flood model. The figure shows three types of model runs. The first type, across the top rows of a and b, shows the results for the combined effects of changes in climate and population. The second type, the RCP runs on the bottom left of a and b, shows the results where climate varies and exposure is fixed. The third type, the SSP runs on the bottom right, shows the results where climate is constant and exposure varies.

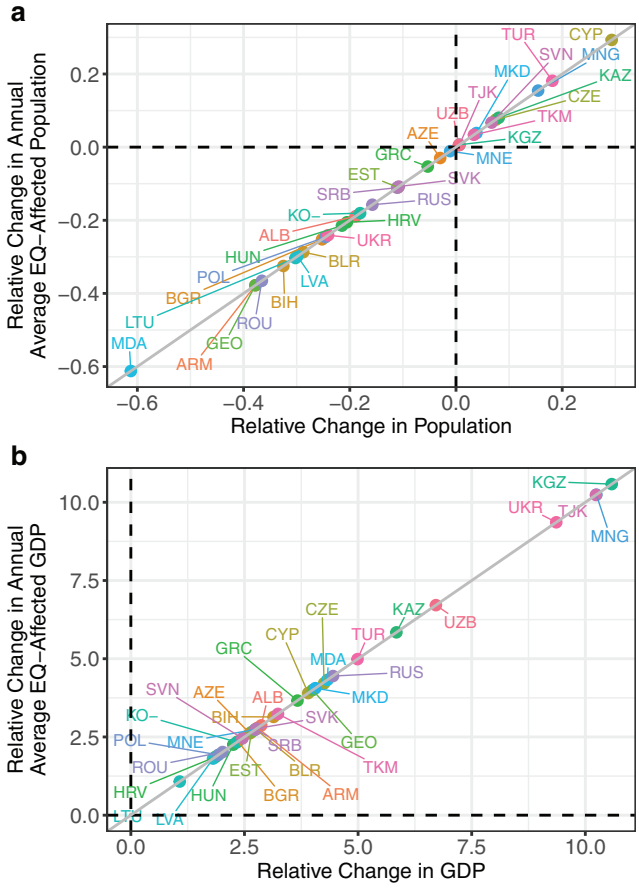

Figure 13. Relative change between 2080 and 2015, $(2080_X - 2015_X)/2015_X$, in annual average population and GDP affected by earthquakes as a function of relative change in population (a) and GDP (b), where X represents population, GDP, annual average affected population or annual average affected GDP. The gray line shows the 1:1 relationship between the relative change in population and annual average EQ-affected population (a) and between the relative change in GDP and annual average EQ-affected GDP (b). The vertical dashed lines denote zero relative change in population (a) and GDP (b) and the horizontal dashed lines denote zero relative change in annual average EQ-affected population (a) and GDP (b). As shown in Figure 1, the mean GDP for all SSPs increases by 2080. As a result, the relative change in GDP is always positive. The results are the average from the five SSPs. The colors are intended to make it easier to distinguish individual countries.

such as river profiles, current flood defenses, local building standards and soil characteristics, as well as more detailed information on exposure, such as the occupancy and construction of local structures, and information on the vulnerability of structures to forces generated by a peril, all of which are incorporated into this study.

The GDP and population affected by floods and earthquakes have been assessed only as a function of hazard and exposure; vulnerability is not taken into account. In other words, GDP and population are considered to be affected once they experience flood water at depths greater than 10 cm or ground motion intensities equal to or greater than MMI VI. In reality, the impact of a flood depends on a variety of factors such as water depth, current velocity and debris, and earthquake impact on factors such as ground motion duration and direction. For example, in reality, the impact of 2 m of flood water is likely to be significantly larger than the impact of 10 cm of flood water. However, the model results will show the same amount of affected GDP for both 2 m and 10 cm flood water.

GLOFRIS, the flood model used for this publication, is a global model that can be used to assess large-scale river flood risks. It does not assess coastal floods, flash floods or urban floods, nor does it consider flood protection measures. Thus, for those areas where flood defenses are present, the model will overestimate the affected GDP and population for return periods lower than the design flood protection level of the existing flood defenses. This in turn leads to an overestimation of the annual average of affected GDP and population. In general, uncertainties in absolute flood risk estimates are large [*Apel et al*., 2008; *Merz et al.* 2008; *DeMoel and Aerts,* 2011], while estimates of relative changes in risk under different scenarios or variability across space are more robust according to *Bupeck et al.* [2011]. A detailed description of the limitations of the GLOFRIS model can be found in *Ward et al*. [2013] and *Winsemius et al*. [2013].

A number of additional caveats are associated with the results that we present. The model results assume no migration of population or GDP. The impact of these assumptions could have a significant impact on the future risk results and the relative changes in risk. Also, we have only considered the primary hazard associated with each peril. Secondary hazards such as liquefaction and/or landslides due to ground motion from an earthquake would increase the hazard and, most likely, risk.

The model results assume a passive response to hazards. People continue to build, live, and work in areas exposed to a hazard and do not improve building practices. With proper planning and construction, risk from hazards can be reduced. One of the best examples of how construction practices can alter the risk from

a hazard is the reduction in urban conflagrations as a result of changes in building practice such as requiring the installation of firewalls and sprinkler systems. Thus, although extreme events such as earthquakes and floods will continue to happen, natural disasters can be minimized through reductions in exposure and vulnerability, and future events such as those shown in Table 1 can be avoided.

5. Summary

A regional flood and earthquake risk assessment was undertaken for 33 countries in the ECA region. The assessment examined current risk (2015) and scenarios for future risk in 2030 and 2080. Flood and earthquake risk were quantified in terms of affected population and affected GDP. Population or GDP were considered to be affected by flooding if a grid cell was affected by a flood of greater than 10 cm, and population or GDP were considered to be affected by an earthquake if a grid cell experienced ground motion equivalent to MMI VI. Earthquake risk was also quantified in terms of fatalities and capital loss.

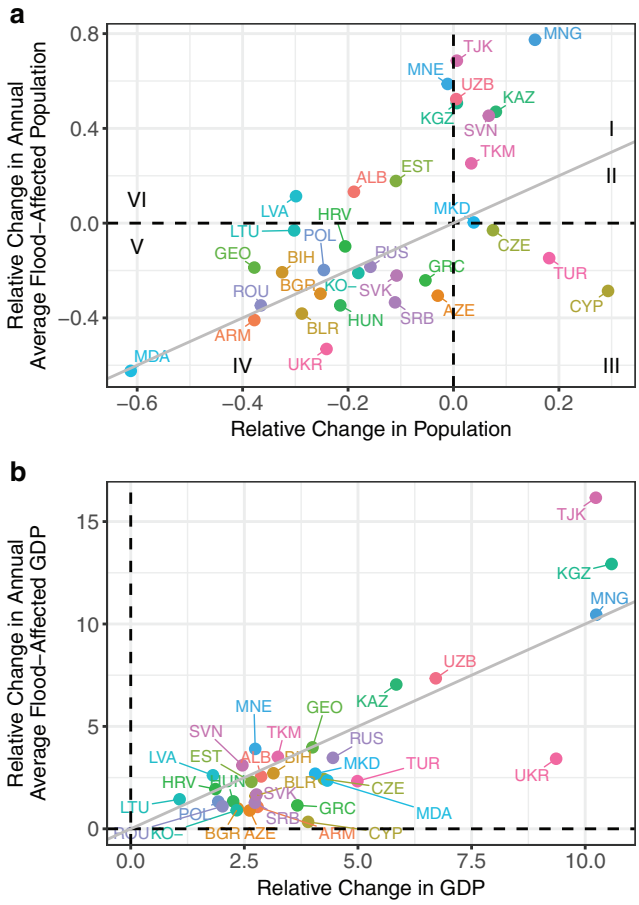

Figure 14. Relative change between 2080 and 2015, $(2080_X - 2015_X)/2015_X$, in annual average population and GDP affected by flood as a function of relative change in population (a) and GDP (b), where X represents population, GDP, annual average affected population, or annual average affected GDP. The gray line shows the 1:1 relationship between the relative change in population and annual average flood-affected population (a) and between the relative change in GDP and annual average flood-affected GDP (b). The vertical dashed lines denote zero relative change in population (a) and GDP (b) and the horizontal dashed lines denote zero relative change in annual average flood-affected population (a) and GDP (b). As shown in Figure 1, the mean GDP for all SSPs increases by 2080. As a result, the relative change in GDP is always positive (b). There is more variability in floods than earthquake (Figure 13) as the spatial distribution of flooding changes in response to climate variation. The model results are the average of the 15 results from all five climate models and the three combinations of SSPs and RCPs. The colors are intended to make it easier to distinguish individual countries. See the text for a discussion of the sectors defined by the dashed and solid lines and labeled by the roman numerals in Figure 14a.

Within the ECA region there is a wide range in average annual population and GDP in 2015 affected by flood and earthquake. As seen in Figure 6, for some countries, e.g., Turkey, earthquake risk is much greater than flood risk. For other countries, e.g., Russia, the situation is reversed. Also, there are other countries that have significant risk from both flood and earthquake. The impact of floods tends to reach a maximum at shorter return periods than that for earthquakes, but this may be due in part to not accounting for flood defenses and because of the binary approach used to account for affected population and GDP.

For 2030 and 2080, national-level changes in population and GDP were distributed spatially as a function of current population and GDP. Estimates of future population and GDP affected by earthquakes vary significantly with population and GDP changes consistent with the SSPs. There is a linear relationship between the relative change in population or GDP and the relative change in earthquake risk. Estimates of future population and GDP affected by floods vary as a function of population and GDP changes consistent with two SSPs and with changes in climate consistent with two RCPs. There is not a linear relationship between the relative change in population and GDP and relative change in flood risk because the flood hazard changes in the future.

Six regions can be specified in the two-dimensional space defined by future relative changes in population or GDP and the relative changes in flood risk to population or GDP at a national level. Positive or negative relative changes in population or GDP each have three regions. Climate change can alter relative flood risk in a manner that either counters, tempers, or enhances the change in relative flood risk expected from a change in exposure. A comparison of the amount of relative change in flood risk for a country could be used to inform decisions regarding countries for further study of the benefits of flood hazard mitigation. However, such decisions will require additional inputs such as information on flood defenses, the vulnerability of the exposure of interest, and higher resolution information on the location of exposures.

Acknowledgments
This work was made possible through the support of the Global Facility for Disaster Reduction and Recovery at the World Bank. Data and code used to generate the figures can be found at https://app.box.com/s/mpnjlyvkzicvu6v97p8of1z839wbu3hn. The earthquake code for this study is not open source. Availability options can be discussed by contacting JED. An updated, open-source version of the flood model, PCRGLOB-WB (backbone of GLOFRIS), is available at https://github.com/UU-Hydro/PCR-GLOBWB_model. However, this is not the version used for this study. The old code is not available as open source. Contact HW for more information on the code's availability. We would like to thank S. Fraser for valuable comments as well as J. C. Gill and an anonymous reviewer whose comments significantly improved the manuscript. JED and HW received funding for the work from GFDRR/World Bank. PJW received additional funding from the Netherlands Organisation for Scientific Research (NWO) via VIDI grant 016.161.324.

References

Albini, P. (2015), *The Great 1667 Dalmatia Earthquake: An in-Depth Case Study*, SpringerBriefs in Earth Sciences, Heidelberg, Germany.

Alcaz, V., A. Zaicenco, and E. Isiciko (2008), Earthquake loss modelling for Seismic risk Management, in *Risk Assessment as a Basis for the Forecast and Prevention of Catastrophies*, edited by I. Apostol, W. G. Coldewey, D. L. Barry and C. Reimer, IOS Press, Amsterdam, 1–11, https://doi.org/10.3233/978-1-58603-844-1-1.

Allen, T. I., and D. J. Wald (2007), Topographic slope as a proxy for global seismic site conditions (VS30) and amplification around the globe, *U.S. Geol. Surv. Open File Rep.*, 2007-1357, 69 pp. [Available at http://pubs.usgs.gov/of/2007/1357/index.html].

Ambraseys, N. (2009), *Earthquakes in the Mediterranean and Middle East*, Cambridge University Press, Cambridge, U. K.

Apel, H., B. Merz, and A. H. Thieken (2008), Quantification of uncertainties in flood risk assessments, *Int. J. River Basin Manage.*, *6*, 149–162, https://doi.org/10.1080/15715124.2008.9635344.

Barabanova, K. (2014), The St. Petersburg Flood of 1824, Environment and Society Portal, *Arcadia, 7, Rachel Carson Center for Environ. and Soc*. [Available at http://www.environmentandsociety.org/arcadia/st-petersburg-flood-1824].

Beek, L. P. H. V., and M. F. P. Bierkens (2008), The global hydrological model PCR-GLOBWB: Conceptualization, parameterization and verification, *Dept. of Phys. Geogr. Rep., Utrecht Univ.*, Utrecht, The Netherlands. [Available at http://vanbeek.geo.uu.nl/suppinfo/vanbeekbierkens2009.pdf].

Beek, L. P. H. V., Y. Wada, and M. F. P. Bierkens (2011), Global monthly water stress: I. Water balance and water availability, *Water Resour. Res.*, *47*, W07517, https://doi.org/10.1029/2010WR009791.

Bouwman, A. F., T. Kram, and K. K. Godewijk (2006), *Integrated Modelling of Global Environmental Change. An Overview of IMAGE 2.4*, Netherlands Environmental Assessment Agency, Hague, the Neth.

Bupeck, P., H. DeMoel, L. M. Brouwer, and J. C. J. H. Aerts (2011), How reliable are projections of future flood damage? *Nat. Hazards Earth Syst. Sci.*, *11*, 3293–3306, https://doi.org/10.5194/nhess-11-3293-2011.

Constantin, A. P., A. Pantea, and R. Stoica (2011), Vrancea (Romania) subcrustal earthquakes: Historical sources and macroseismic intensity assessment, *Roman. J. Phys.*, *56*(5–6), 813–826.

Crichton, D. (1999), The Risk Triangle, in *Natural Disaster Management*, edited by J. Ingleton, Tudor Rose, London, 102–103.

Daniell, J., and A. Schaefer (2014), Eastern Europe and Central Asia Region earthquake risk assessment country and province profiling, *GFDRR/World Bank*. [Available at https://wbg.app.box.com/files/0/f/11669366416/1/f_148268286296].

Daniell, J., F. Wenzel, and A. Schaefer (2016), The economic costs of natural disasters globally from 1900-2015: Historical and normalised floods, storms, earthquakes, volcanoes, bushfires, drought and other disasters, *Geophys. Res. Abstr.*, *18*, EGU2016–EGU1899.

Daniell, J. E. (2014), Development of socio-economic fragility functions for use in worldwide rapid earthquake loss estimation procedures, Doctoral thesis, Karlsruhe Inst. of Technol., Karlsruhe, Germany.

Daniell, J. E., B. Khazai, F. Wenzel, and A. Vervaeck (2011), The CATDAT damaging earthquake database, *Nat. Hazards Earth Syst. Sci.*, *11*, 2235–2251, https://doi.org/10.5194/nhess-11-2235-2011.

Daniell, J. E., F. Wenzel, and B. Khazai (2012), The normalisation of socio-economic losses from historic worldwide earthquakes from 1900 to 2012, in *Proceedings of the 15th World Conference of Earthquake Engineering*, *Paper no. 2027*, Lisbon, Portugal.

Dellink, R., J. Chateau, E. Lanzi, and B. Magné (2017), Long-term economic growth projections in the shared socioeconomic pathways, *Global Environ. Change*, *42*, 200–214, https://doi.org/10.1016/j.gloenvcha.2015.06.004.

DeMoel, H., and J. C. J. H. Aerts (2011), Effect of uncertainty in land use, damage models and inundation depth on flood damage estimates, *Nat. Hazards*, *58*, 407–425, https://doi.org/10.1007/s11069-010-9675-6.

Ebi, K. L., et al. (2014), A new scenario framework for climate change research: Background, process, and future directions, *Clim. Change*, *122*(3), 363–372, https://doi.org/10.1007/s10584-013-0912-3.

European Union, United Nations and World Bank (2014), Serbia Floods 2014, Belgrade, Recovery Needs Assessment. 29 Jun. [Available at http://ec.europa.eu/enlargement/pdf/press_corner/floods/20140715-serbia-rna-report.pdf] .

GFDRR (2016), *The Making of a Riskier Future: How Our Decisions are Shaping Future Disaster Risk*, Global Facility for Disaster Reduction and Recovery, Washington, D. C.

Guha-Sapir, D., R. Below, and P. Hoyois (2016), *EM-DAT: The CRED/OFDA International Disaster Database*, Univ. Catholique de Louvain, Brussels, Belgium. http://www.emdat.be/.

Hallegatte, S., M. Bangalore, L. Bonzanigo, M. Fay, T. Kane, U. Narloch, J. Rozenberg, D. Treguer, and A. Vogt-Schilb (2016), *Shock Waves: Managing the Impacts of Climate Change on Poverty*, World Bank, Washington, D. C.. https://openknowledge.worldbank.org/handle/10986/22787.

Hempel, S., K. Frieler, L. Warszawski, J. Schewe, and F. Piontek (2013), A trend-preserving bias correction – the ISI-MIP approach, *Earth Syst. Dyn.*, *4*, 219–236, https://doi.org/10.5194/esd-4-219-2013.

IPCC (2013), Summary for Policymakers, in *Climate Change 2013: The Physical Science Basis. Contribution of Working Group I to the Fifth Assessment Report of the Intergovernmental Panel on Climate Change*, edited by T. F. Stocker, D. Qin, G.-K. Plattner, M. Tignor, S. K. Allen, J. Boschung, A. Nauels, Y. Xia, V. Bex and P. M. Midgley, Cambridge Univ. Press, Cambridge, U. K.

Liu, C., and R. P. Allan (2013), Observed and simulated precipitation responses in wet and dry regions 1850–2100, *Environ. Res. Lett.*, *8*(3), 034002.

Lomnitz, C. (1974), *Global Tectonics and Earthquake Risk*, Elsevier Scientific Pub. Co., Amsterdam, the Neth.

Merz, B., H. Kreibich, and H. Apel (2008), Food risk analysis: Uncertainties and validation, *Österreichische Wasser- und Abfallwirtschaft*, *60*, 89–94, https://doi.org/10.1007/s00506-008-0001-4.

Murnane, R., A. Simpson, and B. Jongman (2016), Understanding risk: What makes a risk assessment successful? *Int. J. Disaster Resilience Built Environ.*, *7*(2), 186–200, https://doi.org/10.1108/IJDRBE-06-2015-0033.

National Geophysical Data Center / World Data Service (NGDC/WDS) (2017), Significant Earthquake Database, *Natl Geophy Data Center*, NOAA. https://doi.org/10.7289/V5TD9V7K. [Available at https://www.ngdc.noaa.gov/nndc/struts/form?t=101650&s=1&d=1].

O'Neill, B. C. et al. (2012) Meeting Report of the Workshop on The Nature and Use of New Socioeconomic Pathways for Climate Change Research, *Natl. Center for Atmos. Res.*, Boulder, Colo, 2-4 Nov. 2011.

Park, Y.-Y., R. Buizza, and M. Leutbecher (2008), TIGGE: Preliminary results on comparing and combining ensembles, *Q. J. R. Meteorol. Soc.*, *134*(637), 2029–2050, https://doi.org/10.1002/qj.334.

Samir, K. C., and W. Lutz (2017), The human core of the shared socioeconomic pathways: Population scenarios by age, sex and level of education for all countries to 2100, *Global Environ. Change*, *42*, 181–192, https://doi.org/10.1016/j.gloenvcha.2014.06.004.

Sanghi, A., S. Ramachandran, A. de laFuente, M. Tonizzo, S. Sahin, and B. Adam (2011), *Natural Hazards, Unnatural Disasters: The Economics of Effective Prevention*, World Bank Group, Washington, D. C.

Sbeinati, M. R., R. Darawcheh, and M. Mouty (2005), The historical earthquakes of Syria: An analysis of large and moderate earthquakes from 1365 B.C. to 1900 A.D, *Ann. Geophys.*, *48*(3), 347–435, https://doi.org/10.4401/ag3206.

Sinadinovski, C., and K. F. McCue (2013), *50 Years since the Skopje 1963 Earthquake - Implications for Australian Building Standards*, Aust. Earthq. Eng. Soc., Hobart, Tasmania.

Stiros, S. C. (2001), The AD 365 Crete earthquake and possible seismic clustering during the fourth to sixth centuries AD in the eastern Mediterranean: A review of historical and archaeological data, *J. Struct. Geol.*, *23*(2), 545–562, https://doi.org/10.1016/S0191-8141(00)00118-8.

Tenk, A., and L. David (2015), Geographical and GIS analysis of the great flood of 1838 in Pest-Buda, *Geogr. Tech.*, *10*(1), 77–89.

Trenberth, K. E. (2011), Changes in precipitation with climate change, *Clim. Res.*, *47*(1–2), 123–138.

UzReport (2017), Today marks 50 years since earthquake in Tashkent. [Available at http://news.uzreport.uz/news_3_e_141229.html].

van Vuuren, D. P., P. L. Lucas, and H. Hilderink (2007), Downscaling drivers of global environmental change: Enabling use of global SRES scenarios at the national and grid levels, *Global Environ. Change*, *17*, 114130, https://doi.org/10.1016/j.gloenvcha.2006.04.004.

van Vuuren, D. P., et al. (2011), The representative concentration pathways: An overview, *Clim. Change*, *109*(1), 5–31, https://doi.org/10.1007/s10584-011-0148-z.

Ward, P. J., B. Jongman, F. S. Weiland, A. Bouwman, R. vanBeek, M. F. P. Bierkens, W. Ligtvoet, and H. C. Winsemius (2013), Assessing flood risk at the global scale: Model setup, results, and sensitivity, *Environ. Res. Lett.*, *8*(4), 044019.

Weedon, G. P., S. Gomes, P. Viterbo, H. Oesterle, J. C. Adam, N. Bellouin, O. Boucher, and M. Best (2010), *The WATCH Forcing Data 1958–2001: A Meteorological Forcing Dataset for Land Surface- and Hydrological-Models WATCH Technical Report 22*, Met Office Hadley Centre, New Haven, Conn. www.eu-watch.org.

Winsemius, H. C., L. P. H. V. Beek, B. Jongman, P. J. Ward, and A. Bouwman (2013), A framework for global river flood risk assessments, *Hydrol. Earth Syst. Sci.*, *17*, 1871–1892, https://doi.org/10.5194/hess-17-1871-2013.

World Bank, (1998), Tajikistan – Emergency Flood Assistance Project, *The World Bank, World Development Sources, WDS 1998–3*, Washington, D. C.

World Bank (2017) Serbia GDP. [Available at http://data.worldbank.org/country/serbia].